Bipyridyl-Substituted Triazoles as Hole-Blocking and Electron-Transporting Materials for Organic Light-Emitting Devices

Musubu Ichikawa*, Soichi Fujimoto, Yuta Miyazawa, Toshiki Koyama

Department of Functional Polymer Science, Shinshu University, 3-15-1 Tokita, Ueda, Nagano 386-8567, Japan

Norimasa Yokoyama, Tetsuzo Miki

Hodogaya Chemical Co., Ltd., 45 Miyukigaoka, Tsukuba, Ibaraki 305-0841, Japan

Yoshio Taniguchi

Department of Functional Polymer Science, Shinshu University, 3-15-1 Tokita, Ueda, Nagano 386-8567, Japan

Abstract: We have demonstrated bipyridyl substituted triazole derivatives (Bpy-TAZs) as an electron-transporting material for organic light-emitting devices (OLEDs). Substitution of triazole with bipyridyl is a good way to improve electron-transporting ability of triazoles with keeping good hole-blocking ability, which is a useful property of triazole derivatives. A Bpy-TAZ has high electron mobility of above 10^{-4} cm^2/Vs. Moreover, by employing one of Bpy-TAZs as a hole-blocking and electron-transporting material for phosphorescent OLEDs, lower operation voltage was achieved with keeping the same external quantum efficiency of electroluminescence (almost 10%) as compared with the conventional hole-blocking and electron-transporting bilayer consisting of bathocuproine and tris (8-hydroxyquinolinato) aluminum.

Keywords: Amorphous material; Hole blocking; Electron transporting; Triazole; Electroluminescent device; OLED; Phosphorescent device; Mobility; Pyridine

*Corresponding author. Tel: +81-268-21-5498; Fax: +81-268-21-5413; E-mail: musubu@shinshu-u.ac.jp (M. Ichikawa)

1. Introduction

Organic light-emitting devices (OLEDs) have been received much attention due to their potential applications for thin flat television, mobile displays, lightings, optical communication light sources, and so on. OLEDs are generally composed of functionally divided organic multi-layers, e.g., hole transporting (HT), emissive, and electron transporting (ET) layers, and so on.[1, 2] In the last decade, many kinds of amorphous molecular semiconductor materials,[3, 4] working as HT materials[5-9] and ET materials,[10-15] have been proposed, and HT molecular semiconducting materials have become practical due to their high charge carrier mobility and excellent operational durability. On the other hand, there have been scarcely reports on ET organic semiconducting amorphous materials with high performance (high-speed transportation of electrons, easy injection of electrons from the cathode, and good operational durability).[13] Tris (8-hydroxyquinolinato) aluminum(III) (Alq), which is the historical material reported in the first bright OLED by Tang *et al.* in 1987,[16] is still conventionally used as an ET material regardless of its slow electron mobility[17] because it exhibits high operational durability. However, as a reflection of the imbalanced performance between ET and HT materials, electron-feeding from the cathode into an emissive layer controls device characteristics. Consequently, the development of efficient ET organic amorphous semiconducting materials is a challenge of high priority.

Efficient ET materials provide some advantages, such as lowering the operating voltage and power consumption. Moreover, if the ET materials have wide band gaps, in other words, deeper highest occupied molecular orbitals (HOMO), such ET materials can also work as hole blocking (HB) materials. The complete confinement of a hole in an emissive layer by the HB layer raises the quantum efficiencies of electroluminescence (EL). Recently, we have developed a new electron-transporting material family with very high electron mobility: bipyridyl substituted oxadiazoles. The new ET materials show excellent ET properties with electron mobility of above 10^{-3} cm^2/Vs and good thermal stability with high glass transition temperature (Tg) of above 100°C.[18, 19] As the result, using the new materials as electron-transporting materials leaded to lower operation voltage, lower power consumption, and longer lifetime. Consequently, substitution of conventionally well-known electron-transporting molecular skeletons with pyridine and/or bipyridyl will be a valuable way to create new electron-transporting material with high performance. Here we demonstrate another pyridyl substituted material family: bipyridyl

triazoles (Bpy-TAZs), which work as efficient electron-transporting materials and also good hole-blocking materials. In addition, the materials can be utilized for phosphorescent OLEDs.

2. Experimental

2.1 Materials

Figure 1 shows chemical structures of the newly developed materials abbreviated as Bpy-TAZs. These materials are synthesized from the corresponding hydrazide intermediates by ring formation reaction with an aryl amine as shown in Scheme 1. For example, Bpy-TAZ-01 was synthesized from Bpy2-Hyd with 4-*tert*-butylaniline in *o*-dichlorobenzene. The reactions quantitatively proceeded. They were purified by silica gel column chromatography to give white crystals, whose structures were confirmed by ^{1}H-NMR, ^{13}C-NMR, mass spectroscopy and elemental analysis. Further purification was carried out with temperature gradient sublimation in a flow stream of pure argon gas before use. Note that other OLED materials were from industrial companies as sublimation grades, and then used without further purification.

2.2 Synthesis

[2,2']Bipryridinyl-6-carboxylic acid hydrazide (Bpy-Hyd)

[2,2']Bipryridinyl-6-carbonitrile (Bpy-CN) was synthesized from 2,2'-dipyridyl-N-oxide (10.0 g, 58.1 mmol), trimethylsilyl cyanide (8.70 mL, 69.7 mmol) and N,N-dimethylcarbamoyl chloride (6.40 mL, 69.7 mmol) in absolute dichloromethane (100 mL) for 5 days at room temperature by following a previously reported reaction.[18] Note that all regents used in this study were commercially available. Bpy-CN was converted to carboxylic acid with conc. HCl in methanol, and then methyl-esterificated with thionyl chloride in dewatered methanol. Finally, Bpy-Hyd was synthesized from the methyl ester (43.7 g, 204 mmol) with hydrazine (12.8 mL, 408 mmol) in methanol (400 mL). δ_H (270 MHz, $CDCl_3$): 9.12 (1H, s), 8.70 (1H, d, J 4.3 Hz), 8.58 (1H, d, J 7.8 Hz), 8.37 (1H, d, J 8.1 Hz), 8.09 (1H, d, J 7.6 Hz) 7.96 (1H, t, 7.7 Hz), 7.84 (1H, t, J 6.9 Hz), 7.35 (1H, t, J 5.6 Hz), 4.16 (2H, d, J 4.3 Hz).

3,5-Bis([2,2']Bipyridin-6-yl)-4-(4-tert-butylphenyl)-[1,2,4]triazole (BpyTAZ-01)

First, [2,2']Bipyridinyl-6-carboxylic acid N'-([2,2']bipyridinyl-6-carbonyl)-hydrazide (Bpy2-Hyd) was synthesized from Bpy-Hyd (3.70 g, 17.3 mmol) with 4-methylene-oxetan-2-one (7.63 g, 90.8 mmol) in chloroform (139 mL) at the reflux under N_2. After hexane-washing the precipitation obtained by removing chloroform from the solution, Bpy2-Hyd was obtained by a hydrolysis with 70-mL-water of the precipitation (1.45 g) in diglyme (50 mL) at 120°C under N_2. Finally, BpyTAZ-01 was synthesized from Bpy2-Hyd (1.18 g, 2.98 mmol) with 4-*tert*-butylaniline (2.81 mL, 17.9 mmol) in *o*-dichlorobenzene (30 mL) at 100°C for 1 h under N_2 adding phosphorus trichloride (0.286 mL, 3.27 mmol). White powder (0.91 g) of BpyTAZ-01 was obtained by NH-silica-gel chromatography (chloroform:hexane = 2:1). δ_H (270 MHz, $CDCl_3$): 8.58 (2H, d, J 3.8 Hz), 8.40 (2H, dd, J 7.8, 1.1 Hz), 8.31 (2H, dd, 8.1, 1.1 Hz), 7.94 (2H, t, 7.8 Hz), 7.53(2H, dt, 7.6, 1.6 Hz), 7.46 – 7.43 (2H, m), 7.34 – 7.19 (8H, m), 1.27 (9H, s). δ_C (68 MHz, $CDCl_3$): 155.08, 154.85, 154.04, 150.99, 148.59, 146.04, 137.53, 136.24, 134.75, 127.11, 125.49, 124.33, 123.49, 120.83, 120.73, 34.63, 31.43. MS (EI): m/z 509 (M^+). Elemental analysis calculated for $C_{32}H_{27}N_7$: C, 75.42; H, 5.34; N, 19.24. Found: C, 75.63; H, 5.44; N, 18.98.

[2,2']Bipryridinyl-6-carboxylic acid N'-(6-bromopyridine-2-carbonyl)hydrazide (BBH)

First, an intermediate product was synthesized from N,N'-carbonyldiimidazole (29.4 g, 181 mmol) with 6-bromopicolinic acid (35.0 g, 173 mmol) in dewatered acetonitrile (350 mL) for 30 min at 35°C. After cooling the solution to room temperature, add 700 mL acetonitrile and Bpy-Hyd (35.3 g, 165 mmol), and stir the mixture for 3 h at 40°C. BHH white powder (53.2 g) was obtained from the mixture after washing with water and cooled acetonitrile. δ_H (270 MHz, $CDCl_3$): 10.48 (1H, s), 10.23 (1H, s), 8.70 (1H, d, J 4.6 Hz), 8.64 (1H, dd, J 8.0, 1.2 Hz), 8.47 (1H, d, 7.8 Hz), 8.22 (1H, dd, J 7.6, 1.1 Hz), 8.17 (1H, dd, J 7.6, 1.1 Hz), 8.02 (1H, t, J 7.8 Hz), 7.87 (1H, dt, J 7.8, 1.8 Hz), 7.76 (1H, t, J 7.7 Hz), 7.68 (1H, dd, J 8.1, 1.1 Hz), 7.37 (1H, ddd, J 7.5, 4.7, 1.4 Hz).

3-([2,2']Bipyridin-6-yl)-5-[6-(4-tert-butylphenyl)prydin-2-yl]-4-phenyl-[1,2,4]triazole (BpyTAZ-02)

BpyTAZ-Br was synthesized as a shared intermediate product for both BpyTAZ-2 and -3 from BBH with aniline. Initially, aniline (41.2 mL, 452 mmol) and phosphorous trichloride (7.25 mL,

82.9 mmol) in absolute *o*-dichlorobenzine (500 mL) was stirred under nitrogen stream for 1 h at 100°C, and then BBH (30.0 g, 75.3 mmol) was added to the mixture. After that, the mixture was continuously stirred for 1.5 h at 140°C. BpyTAZ-Br was obtained from the mixture by conventional procedures, and then, BpyTAZ-02 was synthesized from BpyTAZ-Br (3.00 g, 6.59 mmol) with 4-*tert*-butylphenylboronic acid (1.76 g, 9.88 mmol) in degassed toluene/ethanol (80mL:20mL) under Ar stream by Suzuki coupling with tetrakis(triphenylphosphine)palladium (0) (0.381 g, 0.329 mmol) and 1-M-K_2CO_3-aquaous solution (22.5 g, 19.8 mmol) for 3 h at 72°C (reflax). After cooling the mixture, precipitation was filtered, washed with water, tolene, and methanol, and then, white powder of BpyTAZ-02 (2.70 g) was obtained by solving and concentrating the precipitation with chloroform. δ_H (270 MHz, $CDCl_3$): 8.58 (1H, d, J 4.0 Hz), 8.37 – 8.35 (2H, m), 8.24 (1H, d, J 7.8 Hz), 7.92 (1H, t, J 7.8 Hz), 7.84 (1H, t, 7.8 Hz), 7.68 (1H, d, J 8.1 Hz), 7.54 – 7.41 (6H, m), 7.31 – 7.19 (5H, m), 7.10 (1H, d, J 8.1 Hz), 1.33 (9H, s). δ_C (68 MHz, $CDCl_3$): 155.85, 155.09, 154.83, 154.27, 152.17, 148.72, 146.53, 146.18, 138.23, 137.63, 137.33, 136.17, 135.19, 129.08, 127.97, 127.80, 126.37, 125.12, 124.13, 123.68, 122.37, 121.22, 120.84, 119.81, 113.65, 34.69, 31.32. MS (EI): m/z 508 (M^+). Elemental analysis calculated for $C_{33}H_{28}N_6$: C, 77.93; H, 5.55; N, 16.52. Found: C, 78.38; H, 5.68; N, 16.26.

3-([2,2']Bipyridin-6-yl)-5-[6-(1-naphthyl)prydin-2-yl]-4-phenyl-[1,2,4]triazole (BpyTAZ-03)

BpyTAZ-03 was synthesized from BpyTAZ-Br (3.00 g, 6.59 mmol) with naphthylene-1-boronic acid (1.70 g, 6.59 mmol) in degassed toluene/ethanol (80 mL:20 mL) under Ar stream by Suzuki coupling with tetrakis(triphenylphosphine)palladium (0) (0.381 g, 0.329 mmol) and 1-M-K_2CO_3-aquaous solution (22.5 g, 19.8 mmol) for 2 h at 72°C (reflax). After cooling the mixture, precipitation was filtered, washed with water, tolene, and methanol, and then, white powder of BpyTAZ-03 (2.12 g) was obtained by recrystallizing from a mixture of tolene and methanol. δ_H (400 MHz, $CDCl_3$): 8.55 (1H, d, J 4.0 Hz), 8.37 (2H, dd, J 7.9, 2.4 Hz), 8.23 (1H, d, J 7.0 Hz), 7.90 (2H, t, J 7.8 Hz), 7.85 (2H, t, J 8.9 Hz), 7.81 (1H, d, J 8.6 Hz), 7.55 (1H, d, J 7.1 Hz), 7.48 – 7.42 (2H, m), 7.41 – 7.36 (2H, m), 7.34 (3H, dt, J 7.4, 7.1, 1.4 Hz), 7.27 (2H, d, J 7.0 Hz), 7.17 (1H, ddd, J 7.5, 4.8, 1.1 Hz), 6.99 (1H, d, J 8.0 Hz), 6.89 (1H, dd, J 7.1, 1.1 Hz). δ_C (101 MHz, $CDCl_3$): 158.33, 155.61, 155.38, 155.10, 154.33, 149.23, 147.46, 146.66, 138.21, 138.13, 137.83, 137.21, 136.64, 134.07, 131.08, 129.27, 129.18, 128.70, 128.66, 128.24, 126.87, 126.07, 125.71,

125.60, 125.37, 124.43, 124.14, 123.29, 121.65, 121.33. MS (EI): m/z 502 (M^+). Elemental analysis calculated for $C_{33}H_{22}N_6$: C, 78.87; H, 4.41; N, 16.72. Found: C, 79.08; H, 4.52; N, 16.39.

2.3 Device Fabrication and Measurements

All OLEDs were fabricated on 150-nm-thick layers of indium-tin oxide (ITO) commercially precoated onto glass substrates with a sheet resistance of 14 Ω/sq. The solvent cleaned ITO surface was treated by O_2-plazma for 5 minutes just before loading the substrates into a high-vacuum chamber (base pressure below ~6×10^{-4} Pa), where organic layers, 0.5-nm-thick LiF, and 200-nm-thick aluminum cathode layers were deposited via thermal evaporation. Deposition rates are, respectively, 0.6 Å/s for organic materials, 0.1 Å/s for LiF, and 6 Å/s for Al. The current density-applied voltage-luminance characteristics of OLEDs were measured with a commercial apparatus (Precise Gauge, EL1003) with a Keithley 2400 source meter.

^{1}H-NMR spectra were recorded either on a JEOL JNM-EX270 spectrometer (270 MHz) or a Bruker AVANCE spectrometer (400 MHz). Elemental analysis was carried out with Yanaco MT-3 CHNcoder. Thermal analysis was performed on Seiko Instruments DSC-6200 at a heating rate of 10°C/min for differential scanning calorimetry (DSC) under nitrogen gas. Ultraviolet (UV) and visible absorption spectra and fluorescence spectra were recorded with a Shimadzu UV-3150 spectrophotometer and a JASCO FP-750 spectrofluorometer, respectively. The highest occupied molecular orbital (HOMO) energy was determined with a Riken Keiki AC-3 photoelectron emission spectrometer, where the HOMO energy was defined as being equal to the ionization potential measured by photoelectron emission spectroscopy. Optical bandgaps were determined by a spectral onset of each UV-vis. absorption spectrum, and then the lowest unoccupied molecular orbital (LUMO) energies were obtained with the HOMO energy and the optical bandgap. The spectroscopic measurements were carried out with thin-films prepared by thermally evaporated on quartz substrates.

Electron mobility was measured by conventional time-of-flight (TOF) technique. 500-ps-duration optical pulse from a nitrogen gas laser (λ=337 nm, Lasertechnik Berlin, MSG-800) was used as an excitation light for TOF. Test samples were prepared by thermal evaporation in vacuum and encapsulated with a fresh desiccant under highly inert atmosphere of N_2 at the dew point of almost –60°C and O_2 concentration of below 10 ppm. We employed a 100-nm-thick

fullerene C_{60} layer as a charge generation layer for the optical excitation.

3. Results and Discussion

3.1 Thermal and Electronic Properties

Figure 2 shows DSC curves of Bpy-TAZ-03. An endothermic peak due to melting was observed at 211°C in a first heating of BpyTAZ-03 powder. A baseline shift due to the glass transition and an exothermic peak at 162°C due to crystallizing were observed in a second heating. The DSC results confirm that BpyTAZ-03 can form a stable glassy state with glass transition temperature (Tg) of 74°C. This Tg value is rather lower than that (94°C) of NPB (see Fig. 5) a practical HT material, but higher than that (64°C) of another generally used HT material TPD (N,N'-diphenyl-N,N'-di(*m*-tolyl)benzidine).

UV-visible absorption and fluorescence spectra of a neat thin film of Bpy-TAZ-03 are shown in Figure 3. The absorption maximum of the material is 304 nm and the material emits bright UV fluorescence. The bandgap of 3.6 eV for Bpy-TAZ-03 from the absorption spectrum is very wide. This wide bandgap characteristics results from the weak π-conjugations of triazole. LUMO level of Bpy-TAZ-03 (2.7 eV) in neat solid is low enough to easily accept electrons from a cathode metal. This nature is caused by substitution of triazole with pyridine. In addition, HOMO level of BpyTAZ-03 (6.3 eV) is sufficiently deep to suppress hole-leakage from the emissive layer to the cathode via the Bpy-TAZ-03 layer, and the hole confinement in the emissive layer leads to high quantum efficiencies of EL. Bpy-TAZ-03 can be utilized as efficient electron-transporting and hole-blocking materials with rather high thermal stability. In addition, the other Bpy-TAZs also show similar absorption-spectroscopic characteristics as presented in the figure. Note that optical interference by the sample thin-film causes broad absorption around 500 – 600 nm.

The thermal and electronic properties of Bpy-TAZs were summarized in Table 1. Only Bpy-TAZ-03 has Tg, and evaporated thin films of Bpy-TAZ-03 have a thermal stability. On the other hand, Bpy-TAZ-01 and 02 have no Tg. No Tg and higher melting points (Tm) of Bpy-TAZ-01 and Bpy-TAZ-02 indicate that they have higher crystallinity than Bpy-TAZ-03. However, high Tm of Bpy-TAZ-01 means that Bpy-TAZs will have good thermal stability; in other words, no decomposition occurs in vacuum evaporation. As we can see from the table,

introduction of asymmetric diversities and a naphthyl substituent gave a good amorphous nature to the materials in common with other amorphous organic semiconductors. Consequently, we believe that it should be successful to obtain another Bpy-TAZ with higher Tg for improving thermal and long-time stabilities of its amorphous state by carrying out some chemical modifications.

3.2 OLED properties

Figure 4 shows current density-voltage (*J*-*V*) characteristics of OLEDs with Bpy-TAZs as electron-transporting materials. The figure also shows reference devices with no Bpy-TAZ. Structures of the devices and used chemicals are shown in Figure 5. As shown in Figure 4, Bpy-TAZs excepting for Bpy-TAZ-01 show higher performance than the TAZ01 reference device: the conventional triazole compound.[20] The Bpy-TAZ-02 device showed comparable *J*-*V* characteristics with the Alq reference device. Therefore, it is concluded that substitution of triazole with pyridyl is a valuable way to enhance the electron-transporting property of triazole derivatives. Furthermore, the Bpy-TAZ-03 device shows higher current efficiency (4.4 cd/A) than the Alq device (3.9 cd/A). This higher efficiency indicates strong hole-blocking nature of the compound. As generally known, hole-blocking is a valuable property of triazoles. Note Bpy-TAZ-01 briefly: the Bpy-TAZ-01 device shows quite bad performance, and we think that the reason must be instability of the amorphous state of Bpy-TAZ-01, not intrinsic inferior natures of electron injection and transport of this molecule, because the Bpy-TAZ-01 layer was completely hazed at the device fabrication, in other words, easily re-crystallized.

As elucidated in the above paragraph, Bpy-TAZs, especially Bpy-TAZ-03, exhibited good performance as not only an electron-transporting material but also a hole-blocking material. So we try to utilize Bpy-TAZ-03 as a double function (electron-transporting and hole-blocking) material. As well known the recent high efficient phosphorescent OLEDs have both hole-blocking layer and electron-transporting layer. In particular, the hole-blocking layer is important to obtain high quantum efficiency because hole-leakage seriously reduces the efficiency. Moreover, it is more important to consider the triplet energy dissipation from the emissive layer to the hole-blocking layer for attaining high quantum efficiency. At present there is only few materials to be utilized as hole-blocking materials for phosphorescent OLEDs, for example,

bathocuproine (BCP), bis (2-methyl-8-quinolinolato) (*p*-phenylphenolato) aluminum (BAlq), and so on.

Figure 6 shows *J-V* characteristics of phosphorescent OLEDs with Bpy-TAZ-03 as a hole-blocking and electron-transporting material, showing together a reference device, where structures of the device and chemicals are shown in Figure 7. As we can see from Figure 6, the phosphorescent OLED with Bpy-TAZ-03 exhibited much lower operation voltage than that of the reference which had a conventional double layer made up with BCP and Alq layers for hole-blocking and electron-transporting functions.[21] Since both devices shows high external quantum efficiency of almost 10 % as shown in the figure, Bpy-TAZ-03 is useful as a hole-blocking and electron transporting materials for phosphorescent OLEDs.

3.3 Electron Mobility

Finally, we would like to briefly discuss electron mobility in Bpy-TAZ-03 thin-film. Figure 8 shows the transient electron photocurrent waveform obtained by TOF measurement. We obtained the transit time (t_T) of 9.70 μs from the transient photocurrent, where t_T was defined as the kink point of the the transient photocurrent. Hence, electron mobility (μ) was determined to be 8.0×10^{-5} cm^2/Vs at the electric field ($E=V/D$) of 680 kV/cm with the following equation:

$$\mu = Dd/(t_T V) \qquad (1),$$

where V, D, and d are, respectively, the applied voltage, the distance between the two electrodes, and the thickness of Bpy-TAZ-03 layer. This mobility is 2-fold higher than that of Alq of 1.3×10^{-6} cm^2/Vs at approximately same electric field from the literature.[22] This high mobility probably caused the better current density-voltage curve of the Bpy-TAZ-03 device than the Alq reference device. In addition, the waveform in Fig. 8 has the well-defined plateau, implying that electron-transportation in Bpy-TZA-03 thin-film is non-dispersive. The degree of carrier transport dispersion can be described by the tail broadening parameter W, defined as[23]

$$W = (t_{1/2} - t_0)/t_{1/2} \qquad (2),$$

where t_0 is the time of the kink and $t_{1/2}$ is the time when the transient photocurrent reaches half of its plateau value. For the transient photocurrent, we calculate W=0.57, indicating a relatively-small dispersion of the electron packet during transport across the sample. As a summary, Figure

9 shows electron mobility *vs.* square root of applied electric field for several materials including Bpy-TAZ-03. As you can see from the figure, Bpy-TAZ-03 shows almost 2-folder higher mobility than Alq for a wide electric field range from 400 to 2000 kV/cm. The mobility is over 10^{-4} cm^2/Vs above 720 kV/cm. This high mobility is comparable to that of a representative ET material with high electron mobility: a silole derivative, 2,5-bis(6'-(2',2''-bipyridyl))-1,1-dimethyl-3,4-diphenylsilole (PyPySiPyPy).[22, 24]

4. Conclusion

In conclusion, we have demonstrated bipyridyl substituted triazole derivatives (Bpy-TAZs) as electron-transporting materials for OLEDs. Substitution of triazole with bipyridyl is a good way to improve electron-transporting ability of triazoles with keeping good hole-blocking ability, which is a useful property of triazole derivatives. By employing Bpy-TAZ-03 as a hole-blocking and electron-transporting material for phosphorescent OLEDs, lower operation voltage was achieved with holding the comparable high external quantum efficiency to the OLED with the conventional BCP/Alq of almost 10 %. At present, the glass transition temperature of Bpy-TAZ-03 is not high enough, but we believe that another Bpy-TAZ with higher Tg should be prepared keeping its high electron mobility by means of some chemical modifications. Now further experiments are in progress.

Acknowledgements

The authors thank Mr. S. Hayashi and Mr. N. Yokoyama of Hodogaya Chem. for helpful advise to the synthesis of the materials, and also thank Dr. Y. Nakajima and Mr. D. Yamashita of Riken Keiki for measuring the ionization potential of compounds with their photoelectron spectroscopic equipment (Riken Keiki AC-3). This work was supported by the Cooperative Link for Unique Science and Technology for Economy Revitalization (CLUSTER) of the Japan's Ministry of Education, Culture, Sports, Science and Technology. It was also supported by the Ministry's 21st Century COE program.

References

[1] C. W. Tang, S. A. VanSlyke, Appl. Phys. Lett. 51 (1987) 913.

[2] C. Adachi, T. Tsutsui,S. Saito, Appl. Phys. Lett. 57 (1990) 531.

[3] Y. Shirota, J. Mater. Chem. 10 (2000) 1.

[4] U. Mitschke, P. Baeuerle, J. Mater. Chem. 10 (2000) 1471

[5] S. A. VanSlyke, C. H. Chen, C. W. Tang, Appl. Phys. Lett. 69 (1996) 2160.

[6] M. Thelakkat, H.-W. Schmidt, Adv. Mater. 10 (1998) 219.

[7] K. Katsuma, Y. Shirota, Adv. Mater. 10 (1998) 223.

[8] H. Tanaka, S. Tokito, Y. Taga, A. Okada, Chem. Commun. (1996) 2175.

[9] M. Ichikawa, K. Hibino, N. Yokoyama, T. Miki, T. Koyama,Y. Taniguchi, Synth. Met. 156 (2007) 1383.

[10] C. Adachi, T. Tsutsui,S. Saito, Appl. Phys. Lett. 55 (1989) 1489.

[11] Y. Hamada, C. Adachi, T. Tsutsui,S. Saito, Jpn. J. Appl. Phys. 31 (1992) 1812.

[12] K. Tamao, M. Uchida, T. Izumizawa, K. Furukawa,S. Yamaguchi, J. Am. Chem. Soc. 118 (1996) 11974.

[13] M. Uchida, T. Izumizawa, T. Nakano, S. Yamaguchi, K. Tamao,K. Furukawa, Chem. Mater. 13 (2001) 2680.

[14] J. Bettenhausen, P. Strohriegl, Adv. Mater. 8 (1996) 507.

[15] S. B. Heidenhain, Y. Sakamoto, T. Suzuki, A. Miura, H. Fujikawa, T. Mor, S. Tokito,Y. Taga, J. Am. Chem. Soc. 122 (2000) 10240.

[16] C. Adachi, S. Tokito, T. Tsutsui,S. Saito, Jpn. J. Appl. Phys. 27 (1988) L269.

[17] R. G. Kepler, P. M. Beeson, S. J. Jacobs, R. A. Anderson, M. B. Sinclair, V. S. Valencia,P. A. Cahill, Appl. Phys. Lett. 66 (1995) 3618.

[18] M. Ichikawa, T. Kawaguchi, K. Kobayashi, T. Miki, K. Furukawa, T. Koyama,Y. Taniguchi, J. Mater. Chem. 16 (2006) 221.

[19] M. Ichikawa, N. Hiramatsu, N. Yokoyama, T. Miki, S. Narita, T. Koyama,Y. Taniguchi, Phys. Status Solidi RRL 1 (2007) R37.

[20] J. Kido, C. Ohtaki, K. Hongawa, K. Okuyama,K. Nagai, Jpn. J. of Appl. Phys. 32 (1993) L917.

[21] M. A. Baldo, S. Lamansky, P. E. Burrows, M. E. Thompson,S. R. Forrest, Appl. Phys. Lett. 75 (1999) 4.

[22] H. Murata, G. G. Malliaras, M. Uchida, Y. Shen, Z. H. Kafafi, Chem. Phys. Lett. 339 (2001) 161.

[23] L. B. Schein, Philos. Mag. B 65 (1992) 795.

[24] S. Tabatake, S. Naka, H. Okada, H. Onnagawa, M. Uchida, T. Nakano,K. Furukawa, Jpn. J. of Appl. Phys. 41 (2002) 6582.

Figure Captions

Figure 1. Chemical structures of Bpy-TAZs.

Figure 2. DSC curves of Bpy-TAZ-03 in first and second heating.

Figure 3. UV and visible absorption spectra of Bpy-TAZs thin-films. The thicknesses of the films are, respectively, 130 nm for Bpy-TZA-01, 90 nm for -02, and 90 nm for -3. PL spectrum of the Bpy-TAZ-03 film was also shown in the figure (right axis).

Figure 4. Current density-voltage characteristics of OLEDs with Bpy-TAZs as electron-transporting materials, showing together the reference devices with Alq and TAZ01

Figure 5. Device structure of OLEDs with different ET materials and chemical structures of materials used.

Figure 6. *J-V* (left axis) and external quantum efficiency (*QE*)-*V* (right axis) characteristics of the phosphorescent OLED with Bpy-TAZ-03 as a hole-blocking and electron-transporting material, showing together a reference device with the conventional structure.

Figure 7. Device structure of phosphorescent OLEDs with Bpy-TAZ-03 as a hole-blocking and electron-transporting layer, and chemical structures of used other chemicals in the OLEDs.

Figure 8. Electron transient photocurrent of TOF measurement of Bpy-TAZ-03 at the applied voltage of 360 V to the Al cathode. The inset shows device structure used.

Figure 9. Electric field dependence of electron mobility of Bpy-TAZ-03, Alq, and PyPySiPyPy. Data for Alq and PyPySiPyPy were referred from the literature by Murata (see text).

Scheme 1. Synthetic routes of Bpy-TAZs.

Table 1. Thermal and electronic properties of Bpy-TAZs

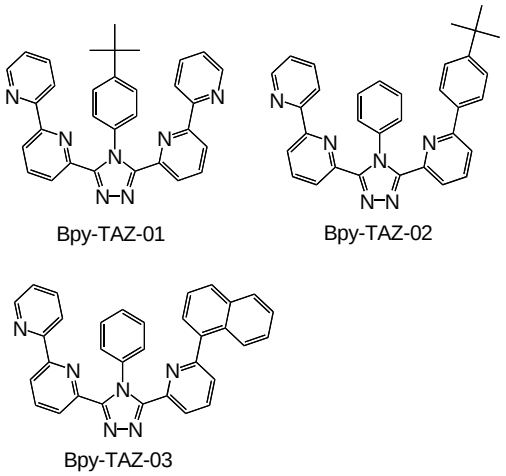

Figure 1. Chemical structures of Bpy-TAZs.

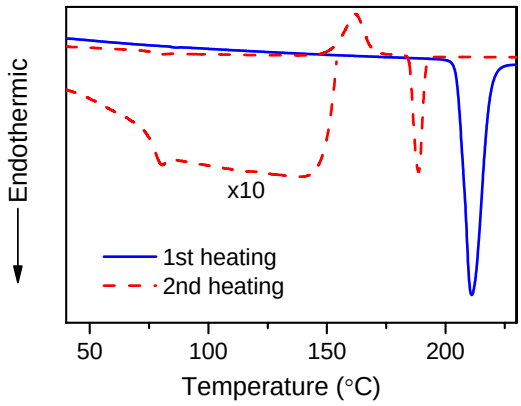

Figure 2. DSC curves of Bpy-TAZ-03 in first and second heating.

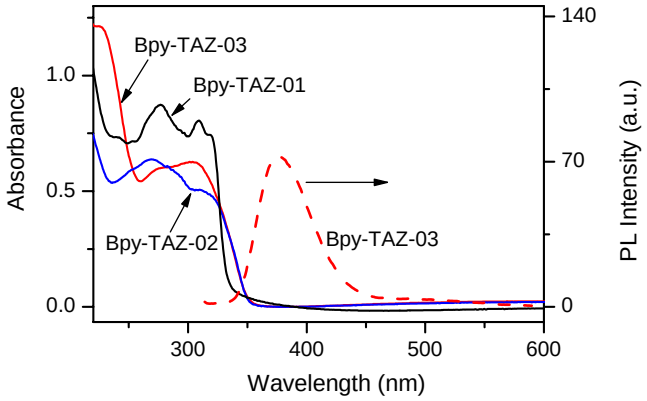

Figure 3. UV and visible absorption spectra of Bpy-TAZs thin-films. The thicknesses of the films are, respectively, 130 nm for Bpy-TZA-01, 90 nm for -02, and 90 nm for -3. PL spectrum of the Bpy-TAZ-03 film was also shown in the figure (right axis).

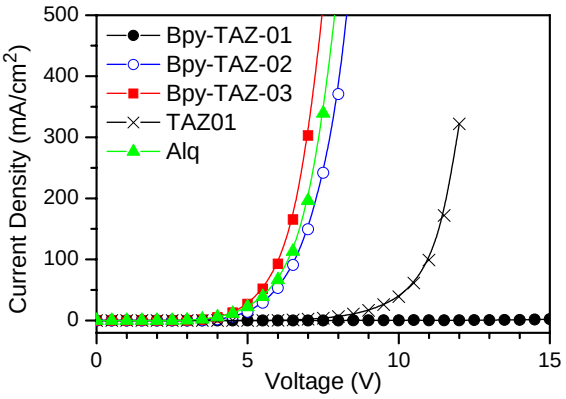

Figure 4. Current density-voltage characteristics of OLEDs with Bpy-TAZs as electron-transporting materials, showing together the reference devices with Alq and TAZ01

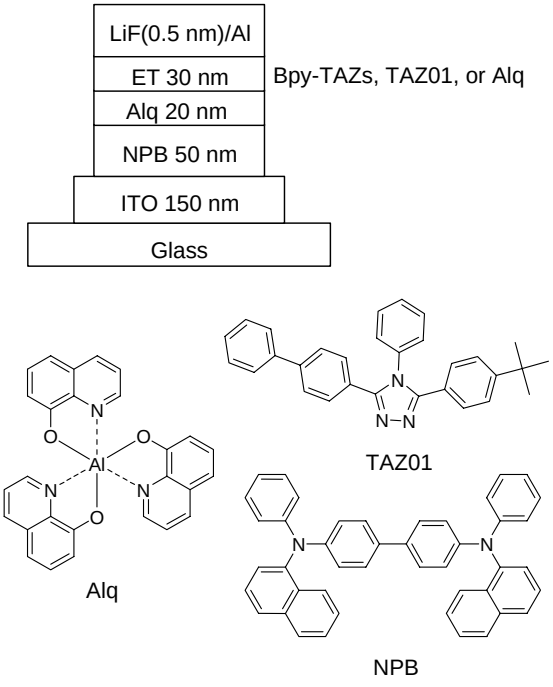

Figure 5. Device structure of OLEDs with different ET materials and chemical structures of materials used.

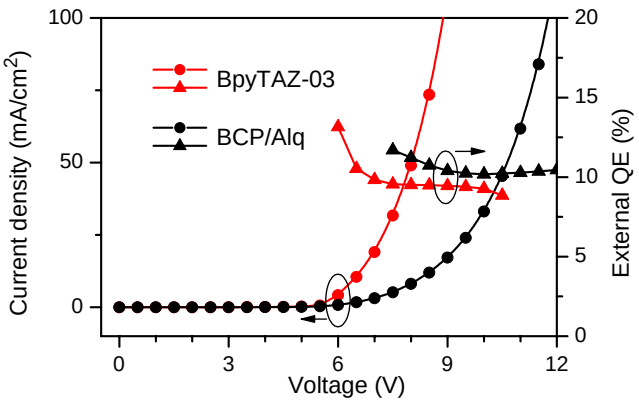

Figure 6. *J-V* (left axis) and external quantum efficiency (QE)-*V* (right axis) characteristics of the phosphorescent OLED with Bpy-TAZ-03 as a hole-blocking and electron-transporting material, showing together a reference device with the conventional structure.

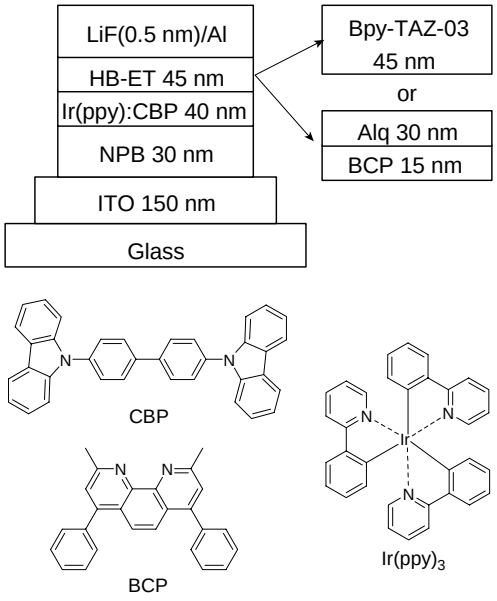

Figure 7. Device structure of phosphorescent OLEDs with Bpy-TAZ-03 as a hole-blocking and electron-transporting layer, and chemical structures of used other chemicals in the OLEDs.

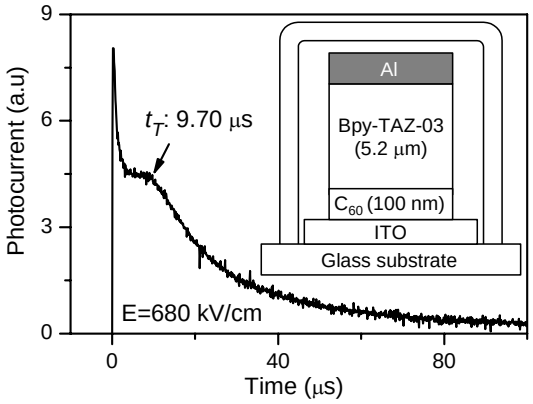

Figure 8. Electron transient photocurrent of TOF measurement of Bpy-TAZ-03 at the applied voltage of 360 V to the Al cathode. The inset shows device structure used.

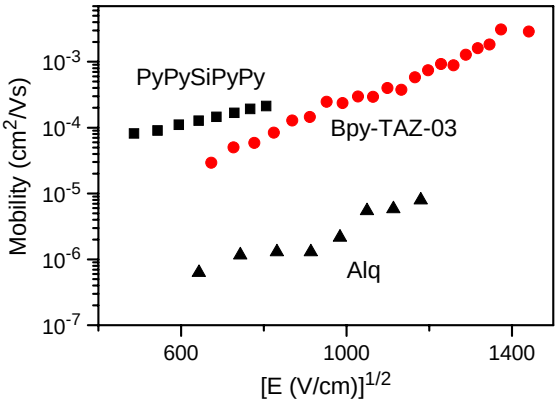

Figure 9. Electric field dependence of electron mobility of Bpy-TAZ-03, Alq, and PyPySiPyPy. Data for Alq and PyPySiPyPy were referred from the literature by Murata (see text).

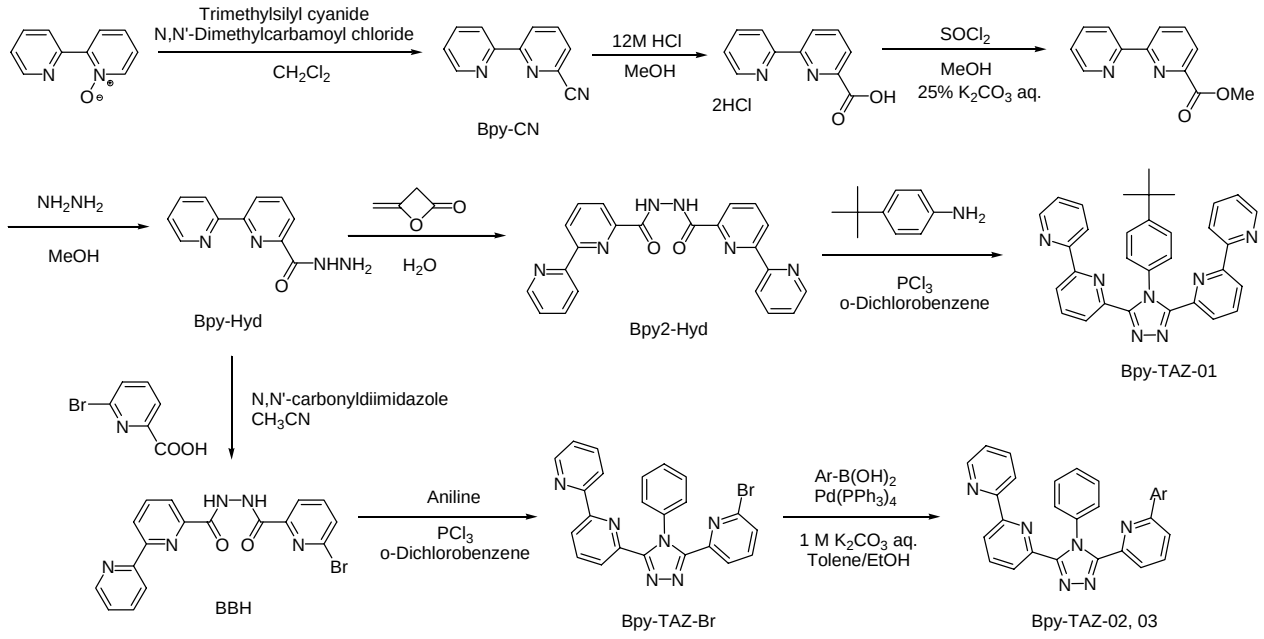

Scheme 1. Synthetic routes of Bpy-TAZs.

Table 1. Thermal and electronic properties of Bpy-TAZs

Bpy-TAZ-	HOMO (eV)	LUMO (eV)	Band Gap (eV)	Tm (°C)	Tg (°C)
01	6.7	2.9	3.8	316	NA
02	6.3	2.7	3.6	268	NA
03	6.3	2.7	3.6	211	74